

## Original Article

# Population divergence in co-distributed Caribbean landfrogs (Eleutherodactylidae: *Eleutherodactylus*) along the Soufrière volcanic slope of Guadeloupe Island, Lesser Antilles

Edward A. Myers<sup>1</sup>, Luigie Alequín<sup>2</sup>, Ayanna Browne<sup>1</sup>, Kevin P. Mulder<sup>1,3</sup>, Danielle Rivera<sup>1,4</sup> , Lauren A. Esposito<sup>2</sup> , Rayna C. Bell<sup>1,\*</sup>, S. Blair Hedges<sup>5,\*</sup>

<sup>1</sup>Department of Herpetology, California Academy of Sciences, San Francisco, CA 94118, USA

<sup>2</sup>Institute for Biodiversity Science and Sustainability, California Academy of Sciences, San Francisco, CA 94118, USA

<sup>3</sup>Wildlife Health Ghent, Faculty of Veterinary Medicine, Ghent University, Merelbeke, Belgium

<sup>4</sup>North Carolina Cooperative Fish and Wildlife Research Unit, Department of Applied Ecology, NC State University, Raleigh, NC 27695, USA

<sup>5</sup>Center for Biodiversity, Temple University, Philadelphia, PA 19122, USA

\*Corresponding authors. Department of Herpetology, California Academy of Sciences, 55 Music Concourse Drive, San Francisco, CA 94118, USA. E-mail: [rbell@calacademy.org](mailto:rbell@calacademy.org); Center for Biodiversity, Temple University, Philadelphia, PA 19122, USA. E-mail: [sbh@temple.edu](mailto:sbh@temple.edu)

## ABSTRACT

Local adaptation to environmental heterogeneity across a landscape can result in population divergence and formation of lineages. On Guadeloupe Island, the active volcano, La Grande Soufrière, peaks at 1460 m a.s.l., with rainforest at low elevations transitioning to humid savannahs at high elevations. Two endemic sister species of *Eleutherodactylus* frogs are co-distributed across this habitat gradient, and previous studies have reported phenotypic differences between lowland and high-elevation populations in each species, in addition to potential ongoing hybridization between the species at high-elevation sites. Here we generate mitochondrial DNA and nuclear DNA genomic data along the elevational transect to quantify population genetic structure, provide historical context for the diversification of these island endemics, and identify potential bottlenecks attributable to the eruptive history of the volcano. We find that both taxa exhibit population clusters that correspond to low- and high-elevation localities; however, genetic divergence is not associated with climate variables or geographical distance. The timing of divergence between the species is estimated at ~3.75 Mya; demographic models indicate low levels of migration between the species after divergence, and we find that ongoing hybridization is likely to be limited. Finally, we find moderate heterozygosity across populations, suggesting that they were minimally impacted by recent volcanic activity. A version of this abstract translated to French can be found in the Supplementary Data. Une version de ce résumé traduite en français est disponible dans les Données Supplémentaires.

**Keywords:** double digest restriction-site associated DNA sequencing (ddRADseq); *Eleutherodactylus barlagnei*; *Eleutherodactylus pinchoni*; elevational gradient; hybrid; population genetics; volcanism

## INTRODUCTION

Environmental heterogeneity can generate population divergence and clinal variation within a species that might eventually lead to the formation of unique evolutionary lineages (Coyne and Orr 1998). Local adaptation to different environmental conditions along such a cline might include a range of phenotypes including ecological selection for background matching and crypsis (Rosenblum 2006), variation in traits associated with intra- or intersexual selection (Stuart-Fox and Ord 2004, Stuart-Fox and Moussalli 2008), or both (Muñoz et al. 2013). A fascinatingly complex aspect of environmental heterogeneity on

volcanic islands is the role that natural disasters can have on resetting parts of ecosystems or entire ecosystems (Dammerman 1929, Feuillet et al. 2002, Markse 2007, Samper et al. 2007), how these might impact genetic diversity and divergence (Carson et al. 1990, Goodman et al. 2012), and, in turn, the ecological and evolutionary trajectories of island communities (Beheregaray et al. 2003). Here we investigate population structure and potential incipient speciation in two co-distributed species of landfrogs (*Eleutherodactylus*) across their elevational range on the volcanically active island of Guadeloupe in the Lesser Antilles.

Received 9 February 2024; revised 23 August 2024; accepted 24 September 2024

© 2024 The Linnean Society of London.

This is an Open Access article distributed under the terms of the Creative Commons Attribution-NonCommercial-NoDerivs licence (<https://creativecommons.org/licenses/by-nc-nd/4.0/>), which permits non-commercial reproduction and distribution of the work, in any medium, provided the original work is not altered or transformed in any way, and that the work is properly cited. For commercial re-use, please contact [reprints@oup.com](mailto:reprints@oup.com) for reprints and translation rights for reprints. All other permissions can be obtained through our RightsLink service via the Permissions link on the article page on our site—for further information please contact [journals.permissions@oup.com](mailto:journals.permissions@oup.com).

The oceanic island of Guadeloupe in the Lesser Antilles archipelago of the eastern Caribbean is composed of two main landmasses, Grande-Terre and Basse-Terre, that have distinct geological origins and are separated by a narrow channel, Rivière Salée, that is ~30–125 m wide and 5 m deep (Fig. 1).

Grande-Terre is a largely flat, limestone plateau that reaches only ~130 m elevation (Cambers 2010). By contrast, the island of Basse-Terre was formed by five major eruptive complexes over the last 3.5 Myr (Feuillet et al. 2002). The highest point is the active volcano, La Grande Soufrière, which peaks at ~1460 m and

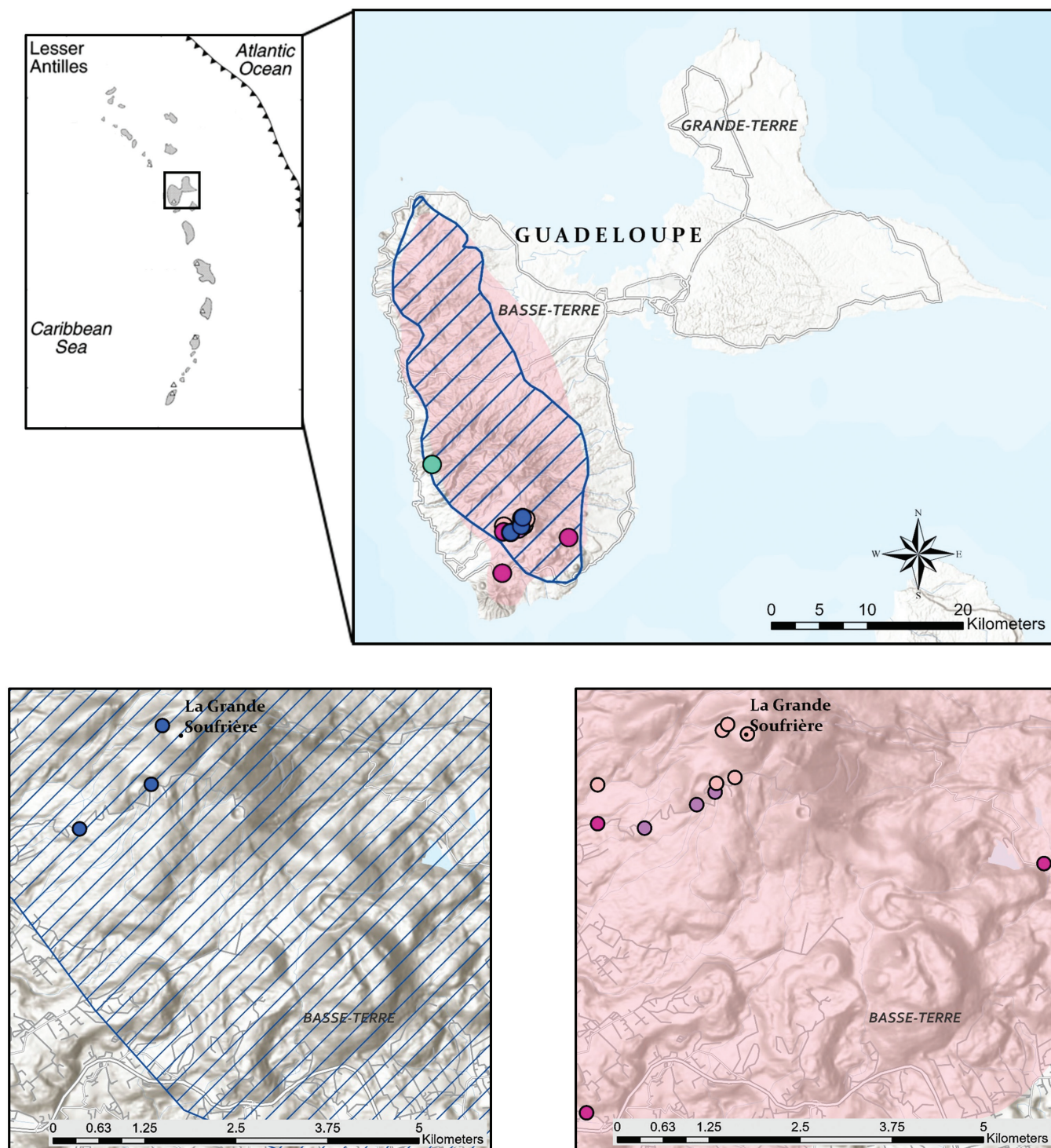


**Figure 1.** Two species of *Eleutherodactylus* frogs are endemic to the island of Guadeloupe, both restricted to the western half of the island (Basse-Terre): *Eleutherodactylus barlagnei* (blue) and *Eleutherodactylus pinchoni* (pink). On the southern side of Basse-Terre lies the active volcano, La Grande Soufrière. Sampling localities are indicated with colours corresponding to genetic clusters within species (see Figs 4, 5). Distribution maps were obtained from the International Union for Conservation of Nature Red List, map layers from Esri, NASA, NGA, USGS, HERE, Garmin, Foursquare, FAO, METI/NAS, and TomTom.

is the highest point of the Lesser Antilles archipelago. The steep topography of Basse-Terre hosts a patchwork of environmental conditions and habitat types over a small geographical area, ranging from lush rainforest at lower elevations to a humid mossy savannah at higher elevations (Imbert *et al.* 1996). La Grande Soufrière last erupted in 1977, resulting in large-scale habitat disturbance and subsequent geological activity including fumaroles and thermal springs that continue to create a harsh environment at the peak (Zlotnicki *et al.* 1992, Massaro *et al.* 2021).

Basse-Terre hosts two endemic species of Caribbean landfrogs: the Guadeloupe stream frog (*Eleutherodactylus barlagnei* Lynch, 1965) and the Guadeloupe forest frog (*Eleutherodactylus pinchoni* Schwartz, 1967). These species are sister taxa (Hedges *et al.* 2008) and are sympatric across Basse-Terre, with distributions that span lowland humid forests to the high-elevation savannahs at the peak of La Grande Soufrière (Fig. 1). *Eleutherodactylus barlagnei* has slightly webbed feet and is strongly associated with torrents and streams, where individuals can be found perched on rocks surrounded by water (Breuil 2002). Even in the high-elevation savannah, *E. barlagnei* individuals shelter under stones near flowing water. Previous authors have noted that the male advertisement calls differ between low- and high-elevation populations of this species, suggesting that there might be additional undescribed species on this island (Hardy 1984, Kaiser 1993). Likewise, differences in coloration, size, and behaviour between lower- and higher-elevation populations of *E. pinchoni* have been noted previously (Hardy 1984). In particular, individuals at high elevation are slightly larger, more darkly pigmented, and live on mossy ground surfaces, whereas individuals at lower elevations are slightly smaller, have more vibrant coloration, and live in humid leaf litter on the forest floor. In addition, male advertisement calls differ between low- and high-elevation populations of *E. pinchoni* (Hardy 1984). The transition between these phenotypes coincides with the elevational transition between humid forest and more open, high-elevation savannah, at which individuals with intermediate phenotypes have been observed (Breuil 2002). Furthermore, some high-elevation individuals exhibit phenotypic characteristics of both *E. barlagnei* and *E. pinchoni*, suggesting that there might be ongoing hybridization between these species (Breuil 2002). Guadeloupe also hosts two additional species of *Eleutherodactylus*: the Lesser Antillean frog (*Eleutherodactylus johnstonei* Barbour, 1914), which observations (Hedges 1989) and genetic data (Yuan *et al.* 2022) indicate to be an introduced species on the island, and the Martinique frog [*Eleutherodactylus martinicensis* (Tschudi, 1838)], whose native vs. introduced status across its extensive distribution in the Lesser Antilles has not yet been clarified thoroughly with genetic data (Kaiser 1992).

Here we used genetic data to investigate the evolutionary history of endemic landfrogs on Guadeloupe and to characterize contemporary patterns of genetic diversity across an elevational transect. Specifically, we test the hypothesis that in both *E. barlagnei* and *E. pinchoni*, populations at high and low elevations along La Grande Soufrière are genetically distinct. In addition, we compare patterns of genetic diversity between higher- and lower-elevation populations to test for potential population bottlenecks in response to volcanic activity and the potential for hybridization between the species at high elevations,

as suggested by Breuil (2002). We discuss the results of these genetic analyses with respect to transitions in environment and phenotype (advertisement call and coloration) along this elevational transect that have been noted by previous authors.

## MATERIALS AND METHODS

### Data generation and bioinformatics

We obtained 114 tissue samples (20 *E. barlagnei* and 94 *E. pinchoni*) collected from the southwest side of Guadeloupe in 1984 (Fig. 1) and three *E. martinicensis* to include as an outgroup. One of these individuals (SBH 102142) was identified as a potential *E. barlagnei* × *E. pinchoni* hybrid in the field. We extracted DNA using protein precipitation (Qiagen, Valencia, CA, USA), eluted DNA in 100 µL of distilled H<sub>2</sub>O, and quantified extractions with QUBIT v.2.0 (Thermo Fisher Scientific, Waltham, MA, USA). All samples were cleaned using sparQ magnetic beads (Quantabio) to remove any inhibitors that might affect enzymatic activity. We sequenced the cytochrome b mitochondrial gene using newly designed primers that sit inside the target region sequenced in previous studies of *Eleutherodactylus* (Velo-Antón *et al.* 2007) for a target sequence length of 782 bp: EleuthGuade\_93F: TTGAYCTCCCMACACCMKCW; and EleuthGuade\_729R: CCGAYAGCGTCTTTRTATGWR. Genomic DNA was amplified using 0.2 µL of Invitrogen DreamTaq following the manufacturer's guidelines in 25 µL reactions, adding 0.5 µL of each primer, 1 µL of MgCl<sub>2</sub>, 3.5 µL of Dream Buffer, and 0.5 µL of bovine serum albumin. PCRs were run for 50 cycles with an annealing temperature of 48°C (94°C for 45 s, 49°C for 30 s, and 72°C for 55 s) and final extension for 2 min at 72°C. Amplified PCR products were cleaned using ExoSAP-IT (United States Biochemical), and cleaned amplicons were sequenced using the BigDye Terminator Cycle Sequencing (Applied Biosystems) by ElimBio (Hayward, CA, USA). DNA sequences were edited in GENEIOUS PRIME v.2022.2.2.

We generated a double-digest restriction site-associated DNA (ddRAD; Peterson *et al.* 2012) dataset for a subset of the specimens from each locality. These ddRAD libraries were prepared following a modified protocol by Peterson *et al.* (2012) as published by Grant *et al.* (2022). Approximately 3000 ng of genomic DNA was digested using the restriction enzymes SphI and EcoRI (NEB, Ipswich, MA, USA) for 3 h at 37°C. Samples were ligated to a universal P2 adapter, and 24 uniquely barcoded P1 adapters were used. Following the ligation step, samples were combined in pools of eight, and a bead clean-up step was performed. Libraries were size selected for 400–600 bp using the Blue Pippin (Sage Science, Beverly, MA, USA) 2% gel cassettes and the internal V1 marker. The size selected pools were amplified for 8–10 cycles using TruSeq 8 bp Unique Dual Index (UDI) barcodes on both primers to catch and remove potential index hopping (Costello *et al.* 2018). Samples were sequenced on a partial Illumina NovaSeq S4 run with 150 bp paired-end reads at the UC Davis DNA technologies core facility, with a sequencing depth ranging from 0.048 to 15.5 (mean = 5.8) million reads per sample.

We processed the raw Illumina reads with IPYRAD v.0.9.92 (Eaton and Overcast 2020) using the *de novo* paired ddRAD pipeline. Reduced representation sequencing has revolutionized

the field of systematic biology and population genetics (Carstens et al. 2012). However, careful considerations of data analysis are needed to confirm that homologous loci are being assembled (Harvey et al. 2015), particularly within taxa with large repetitive genomes, such as amphibians. Of particular interest is the clustering threshold set for RADseq-like data assembly, which will determine how divergent two sequence reads can be to merge them into the same homologous locus rather than splitting true homologous reads into paralogous loci. The choice of clustering thresholds can result in very different datasets and will ultimately influence biological inferences for empirical systems (Harvey et al. 2015, Rodriguez-Ezpeleta et al. 2016, Shafer et al. 2017). Most parameters in IPYRAD were left as default; however, we tested 11 different clustering thresholds ranging from .88 to .98 for the intraspecific datasets and from .88 to .98 at even intervals for six different thresholds for the interspecific dataset. These clustering thresholds span a range from potentially over-splitting natural allelic variation to lumping paralogous loci (McCartney-Melstad et al. 2019).

After applying IPYRAD filters for potentially paralogous loci, it is possible to examine the relationship between the clustering threshold and the percentage of clusters retained, where the expectation is that there will be a positive relationship between increased clustering threshold values and the percentage of retained clusters. Here, the optimal threshold for retaining true homologues should be in the shallow declining slope of the relationship between these two variables (McCartney-Melstad et al. 2019). Finally, estimated levels of heterozygosity can also help to determine optimal clustering thresholds. For example, thresholds set too low will result in clustering of paralogous loci, which will then be discarded in further filtering; this will ultimately lead to increased levels of estimated heterozygosity with higher clustering thresholds. The recommendation is that the optimal clustering threshold will result in the maximum level of estimated heterozygosity (McCartney-Melstad et al. 2019). The estimated sequencing error rate can also be used to help determine the best clustering thresholds (as has been suggested by the developers of IPYRAD; [https://ipyrad.readthedocs.io/en/0.9.93/assembly\\_guidelines.html](https://ipyrad.readthedocs.io/en/0.9.93/assembly_guidelines.html)).

Thus, to determine the best clustering threshold for the data, we used three metrics: the percentage of non-paralogues after filtering (McCartney-Melstad et al. 2019); the level of heterozygosity per sample (Ilut et al. 2014) from step 5 in IPYRAD; and the estimated sequencing error rate reported after running IPYRAD step 7. All these metrics are accessible from IPYRAD outputs at steps 5 and 7 and do not require further processing of genetic data, making the evaluation of numerous thresholds straightforward across a broad range of taxa. To estimate the percentage of non-paralogues, we first calculated the total number of clusters after filtering by depth ( $\text{hidepth\_clusters} = \text{clusters\_total} - \text{filtered\_by\_depth}$ ), then the percentage of non-paralogous clusters  $\{ \% \text{non-paralogues} = [\text{hidepth\_clusters} - (\text{filtered\_by\_maxH} + \text{filtered\_by\_maxAlleles})] / \text{hidepth\_clusters} \}$  in base R (R Core Team 2008). Finally, we used the estimated error rate (`error_est` in the final statistics file) to evaluate the cluster threshold; the known Illumina NovaSeq error rate is ~.001 (Stoler and Nekrutenko 2021); we therefore selected the clustering threshold with the closest error to this value as

estimated in IPYRAD (Eaton and Overcast 2020; [https://ipyrad.readthedocs.io/en/0.9.93/assembly\\_guidelines.html](https://ipyrad.readthedocs.io/en/0.9.93/assembly_guidelines.html)).

After determining the best clustering thresholds for these datasets based on a combination of all three criteria (96%; Supporting Information, Fig. S1), we filtered the single nucleotide polymorphism (SNP) matrices further, to allow no more than 50% missing data at each locus using VCFTOOLS (Danecek et al. 2011). Samples were dropped if they were sequenced for <50% of the retained loci, and we retained one SNP per locus for all population genetic analyses, resulting in 17 748 SNPs across 44 individuals for the combined dataset, 18 217 SNPs for eight samples in the *E. barlagnei*-only dataset, and 21 627 SNPs across 36 samples for the *E. pinchoni*-only dataset.

### Mitochondrial DNA phylogenetic and dating analysis

We used IQ-TREE v.2.1.3 (Minh et al. 2020) to estimate a mitochondrial DNA (mtDNA) gene tree of all sequenced individuals, with 1000 ultrafast bootstraps to assess support (Hoang et al. 2018). We used MODELFINDER, implemented in IQ-TREE (Kalyaanamoorthy et al. 2017), to select the best-fitting model of nucleotide evolution for the mtDNA sequence data. For outgroups, we used the three *E. martinicensis* sequenced in the present study and three *E. johnstonei* (GenBank accessions OM928288–OM928290).

To estimate a time-calibrated mtDNA gene tree, we used BEAST v.2.6.7 (Bouckaert et al. 2019), following the calibration used in previous analyses of Lesser Antillean *Eleutherodactylus* (Heinicke et al. 2007, Yuan et al. 2022). Two mtDNA sequences of both *Eleutherodactylus* species (*E. barlagnei* and *E. pinchoni*; one from a high-elevation and one from a low-elevation collecting site), in addition to the outgroups *E. martinicensis* (this study), *E. johnstonei* (GenBank accession OM928290), and *Eleutherodactylus cooki* Grant 1932 (GenBank accession HQ831648), were aligned using MUSCLE (Edgar 2004). We then used jMODELTEST2 (Darriba et al. 2012) to determine the best-fitting model of sequence evolution using the Akaike information criterion; this model was then implemented in the BEAST analysis. With BEAST, we used a birth–death prior, a random local clock, and a log-normally distributed calibration for the divergence between *E. martinicensis* and *E. cooki* (16.9 Mya; 11.6–24.4 Mya) that was previously estimated from fossil and geological calibrations (Heinicke et al. 2007). The Markov chain Monte Carlo chain was run for  $2.5 \times 10^7$  iterations, sampling every 2500 iterations. To evaluate convergence, we examined TRACER plots and estimated effective sample sizes of parameters in TRACER v.1.7 (Rambaut et al. 2018). Using TREEANNOTATOR (Bouckaert et al. 2019), 10% of the posterior sample was removed, and a consensus gene tree was estimated.

### Population clustering and genetic diversity

To conduct a discriminate analysis of principal components, we used the *adegenet* package in R (DAPC; Jombart 2008). This was performed first with both taxa grouped together, then separately for each species to assess whether there is evidence of interspecific gene flow (e.g. hybridization) and to quantify intraspecific genetic structure. Akaike information criterion scores were used to determine the number of ancestral populations (*K*) in all three analyses. Additionally, we used principal component analysis

(PCA) implemented in *adeigenet* to visualize genetic variation and population clustering between and within these two species. To ensure that missing data were not biasing clustering results, we removed all missing data from the interspecific dataset using VCFTOOLS (Danecek *et al.* 2011) and reran a PCA. For the intraspecific analyses, we plotted principal component (PC) 1 of genetic variation against the elevation at which each sample was collected. We estimated individual-level heterozygosity in the R package *popgenstuff* v.0.0.0.9 (Bradburd 2012; <https://github.com/gbradburd/popgenstuff>) using the individual species datasets, and then, using linear regression in R, tested for a correlation between heterozygosity and the elevation of the collecting locality.

To visualize the extent of admixture between the two species and assess population structure within species, we used the R package *LEA* to run sparse non-negative matrix factorization (sNMF; Frichot *et al.* 2015). The sNMF analysis was run on the combined dataset, *E. barlagnei*-only dataset, and *E. pinchoni*-only dataset, for  $K = 1-4$ , using 100 repetitions for each value of  $K$ , 100 iterations of the sNMF algorithm, and the default  $\alpha$  value. The  $K$  value was determined using cross-entropy scores.

Lastly, we constructed a haplotype network based on the mtDNA for each species using the R package *pegas* (Paradis 2010). Individuals within these networks were colour-coded according to the elevation (low/high for *E. barlagnei*; low/medium/high for *E. pinchoni*) at which they were collected.

### Isolation by distance and environment

We tested for associations between genetic distances and geographical distances [a pattern of isolation by distance (IBD)] and between genetic distances and environmental distances [isolation by environment (IBE)]. For IBD, we calculated genetic distances between collection sites using the R package *adeigenet* (Jombart 2008) and geographical distances between sites with *fossil* (Vavrek and Matthew 2011). A Mantel test was then conducted between these two distance matrices using the R package *ade4* (Dray and Dufour 2007). Additionally, we tested for both IBD and IBE using generalized dissimilarity modelling (GDM; Ferrier *et al.* 2007). This matrix regression technique models associations between distance matrices and fits non-linear relationships between these matrices (Ferrier *et al.* 2007). For example, this method can test for correlations between the dependent variable (genetic differentiation) and numerous independent variables, such as annual mean temperature, annual precipitation, and geographical distances (García-Rodríguez *et al.* 2021). Climate data were extracted from the 19 Chelsa Bioclim variables (Karger *et al.* 2017) for each collecting locality. We then fitted generalized dissimilarity models with the *gdm* R package (Manion *et al.* 2016), performing 100 matrix permutations for model and variable significance testing.

### Diversification and population demographic history

To understand the context of *in situ* diversification for these island endemic frogs, we used the program GADMA v.2.0 (Noskova *et al.* 2023) to estimate gene flow and changes in population size since initial divergence. GADMA uses a genetic algorithm to assess historical demography without prespecifying a model of population divergence. This analysis was run twice,

once with all samples and again with the removal of individual SBH 101896, which was found to be admixed between the two species. We converted the unlinked SNP data in .vcf format to the folded site frequency spectrum (SFS) using EASYSFS (<https://github.com/isaacovercast/easySFS>), downsampling *E. barlagnei* to four diploid samples and *E. pinchoni* to 16 diploid samples to average over possible resampling schemes and construct a more complete data matrix. Although sample sizes were uneven between the two species, it has been demonstrated that the accuracy of SFS-based analyses is contingent on the number of segregating sites, and including more individuals does not increase this accuracy (Terhorst and Song 2015). We therefore follow the suggestion by Noskova *et al.* (2020) in considering the limitations of such approaches by implementing a simplified demographic model. Within GADMA, we used the *moments* engine (Jouganous *et al.* 2017) and allowed asymmetric migration rates, specified an initial and final structure with one time period per divergence (i.e. 1,1), and used 100 optimizations of the genetic algorithm to arrive at the final demographic model. Genome-wide mutation rates are largely unknown in amphibians; therefore, we ran GADMA without a mutation rate, which allowed us to infer a model in which these two taxa would have diverged with relative scales for divergence time, effective population sizes, and migration rates.

## RESULTS

### Mitochondrial DNA phylogenetic and dating analysis

The best-fitting model of sequence evolution for the cytochrome b alignment is GTR+G+I, and the maximum likelihood gene tree inferred from IQ-TREE strongly supports *E. barlagnei* and *E. pinchoni* as sister species (bootstrap support = 100; Fig. 2). Divergence dating analyses in BEAST indicate that *E. barlagnei* and *E. pinchoni* diverged from one another 3.75 Mya (95% highest posterior density 1.91–5.82 Mya; Fig. 2). Divergence times estimated between high- and low-elevation populations in each species are ~0.46 Mya (95% highest posterior density 0.09–0.93 Mya for *E. barlagnei* and 0.05–0.97 Mya for *E. pinchoni*).

### Population clustering and genetic diversity

The DAPC results of the combined dataset identify three distinct groups, with clear separation between the species (Fig. 3A). These groups are also identified in the sNMF analysis (Fig. 3B), with the eight individuals identified in the field as *E. barlagnei* having >90% assignment to one population cluster (shown in blue in Fig. 3B). The 36 remaining individuals were all identified in the field as *E. pinchoni* and exhibit >90% assignment to one of the other two population clusters (pink clusters in Fig. 3B). The only exception is sample SBH 101896, which exhibits intermediate assignment probabilities to all three genetic groups (Fig. 3B). This individual is also intermediately placed in PC space when clustering both species (Fig. 3A). In the PCA with no missing data (2503 SNPs), the assignment of sample SBH 101896 is identical to the PCA inferred from a dataset with missing data (Supporting Information, Fig. S2). We examined the morphological voucher specimen (USNM 565006) to assess whether it displays traits of one or both species as described by Schwartz (1967; *E. barlagnei* has a larger snout-vent length,

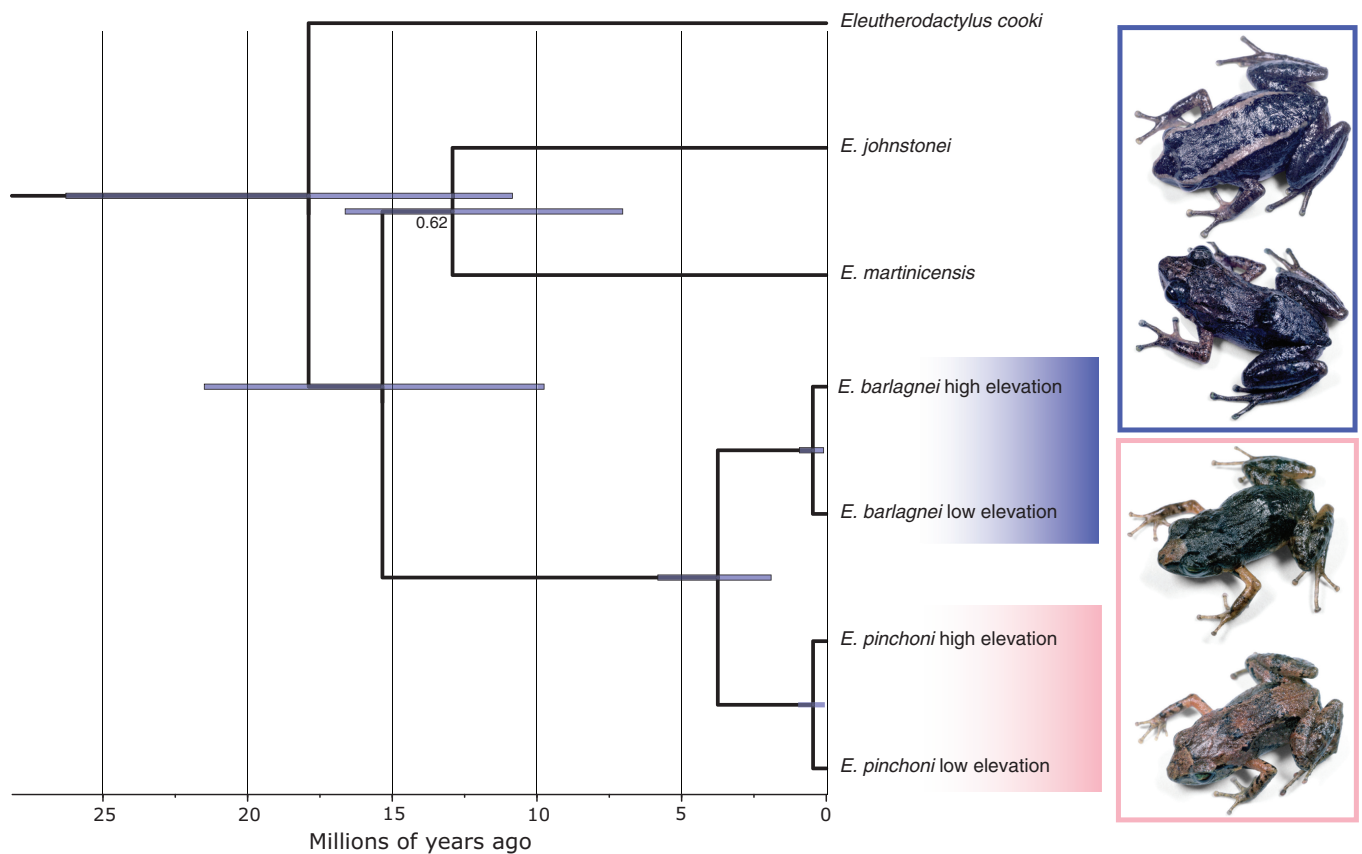


**Figure 2.** Divergence times estimated from mitochondrial DNA sequence data in BEAST. All nodes are supported with a posterior probability of 1.0 unless otherwise noted. Blue bars at nodes represent the 95% highest posterior density of estimated divergence times. Photographs on the right, from top to bottom, are *Eleutherodactylus barlagnei* from a high-elevation site, *E. barlagnei* from a low-elevation site, *Eleutherodactylus pinchoni* from a high-elevation site, and *E. pinchoni* from a low-elevation site.

webbed feet, and an overall lack of colour pattern). We found that this potential hybrid is a male with a snout–vent length of 18.3 mm, a chevron dorsal colour pattern, and lack of webbing between the toes, all morphological traits consistent with *E. pinchoni*. By contrast, the individual identified in the field as a potential *E. barlagnei* × *E. pinchoni* hybrid (SBH 102142) exhibits clear assignment to *E. pinchoni* in analyses of nuclear DNA (nuDNA) and has an *E. pinchoni* mtDNA haplotype.

Within *E. barlagnei*, the DAPC results identify two distinct groups (Fig. 4A) that correspond to samples from low (120 m) and high (950–1325 m) elevations (Fig. 4B). These groups are also identified in the sNMF analysis (Fig. 3C), with all individuals exhibiting limited admixture. Within *E. pinchoni*, the DAPC results identify two groups (Fig. 5A) that form a gradual transition from low (337 m) to high (1460 m) elevation (Fig. 5B). The sNMF analysis, however, identifies three distinct clusters with extensive admixture (Fig. 5C). Samples assigned to the first group in sNMF (>75%) were collected at lower elevations (337–685 m; dark pink in Fig. 5), those assigned to the second group at intermediate elevations (950–980 m; medium pink in Fig. 5), and those in the third group at higher elevations (1100–1460 m; light pink in Fig. 5). The fully sampled phylogeny and haplotype networks reveal distinct lineages and haplotype groups in each species. In *E. barlagnei*, we do not find shared haplotypes among low- and high-elevation sampling localities (although the haplotypes are not clearly structured by elevation), whereas in

*E. pinchoni* we find extensive haplotype sharing across all sampling sites (Figs 4D, 5D; Supporting Information, Fig. S3).

Genome-wide estimates of heterozygosity for *E. barlagnei* individuals range from .15 to .30, and within *E. pinchoni* heterozygosity ranges from .09 to .12. Heterozygosity was not correlated with elevation in either species ( $P = .09$  in *E. barlagnei*;  $P = .92$  in *E. pinchoni*).

#### Isolation by distance and environment

We do not find support for IBD using a Mantel test in either *E. barlagnei* ( $P = .07$ ) or *E. pinchoni* ( $P = .06$ ), suggesting that geographical distance between sampled localities does not have a significant influence on genetic variation. Generalized dissimilarity models indicate geographical distance, mean diurnal air temperature range (bio2), and isothermality (bio3) as potential predictors of genetic distance within *E. barlagnei*; however, this model is not significantly supported in permutation analyses ( $P > .05$ ). Within *E. pinchoni*, GDMs indicate mean diurnal air temperature range (bio2), isothermality (bio3), annual range of air temperature (bio7), and amount of precipitation in the wettest month (bio13) as potential predictors of genetic distance; however, this model is also not significant ( $P > .05$ ).

#### Population demographic history

The GADMA analysis without the admixed sample converges on a model with gradual population size growth in both species and

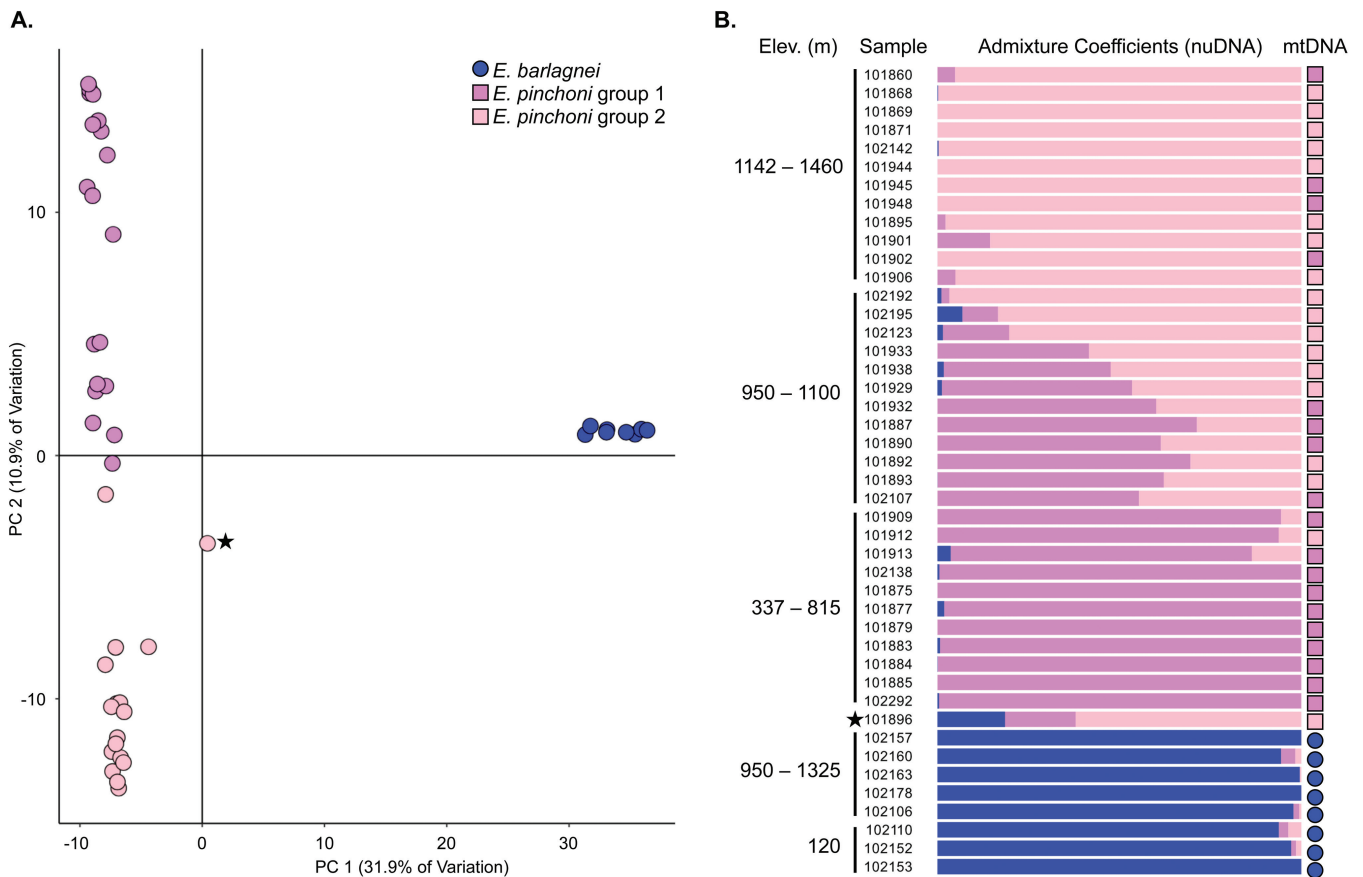


**Figure 3.** A, principal components (PC) analysis for the combined dataset (17 748 single nucleotide polymorphisms) including both *Eleutherodactylus barlagnei* (blue dots) and *Eleutherodactylus pinchoni* (pink dots) as identified in the combined dataset discriminate analysis of principal components. B, sparse non-negative matrix factorization barplot depicting admixture coefficients for each specimen of *E. barlagnei* and *E. pinchoni* and its corresponding mitochondrial DNA haplotype (for complete mitochondrial DNA results, see [Supporting Information, Fig. S3](#)). Within species, the samples are ordered by sampling locality elevation (see [Supporting Information, Appendix](#)), with the exception of SBH 101896, which had intermediate assignment to *E. barlagnei* and *E. pinchoni* and was collected at 1142 m elevation. This sample is indicated with a star in both panels. Abbreviations: Elev., elevation; nuDNA, nuclear DNA.

limited, asymmetric migration between the two species, with more migrants per generation from *E. pinchoni* to *E. barlagnei* (Fig. 6). The analysis that included the admixed sample converges on a similar demographic history, but with no population growth in *E. barlagnei* and with a higher rate of migration from *E. barlagnei* to *E. pinchoni* ([Supporting Information, Fig. S4](#)).

## DISCUSSION

### *In situ* diversification of the endemic landfrogs of Guadeloupe

The island of Guadeloupe has a complex geological history, with two major landmasses, Grande-Terre and Basse-Terre, that have distinct origins and present-day environmental conditions. The endemic frogs of the island are restricted to the more humid, western half of the island, Basse-Terre, which was formed over the last 3.5 Myr ([Feuillet et al. 2002](#)). Phylogenetic analyses of Caribbean *Eleutherodactylus* indicate that the two Guadeloupe endemics are sister species ([Hedges et al. 2008](#), [Yuan et al. 2022](#)) and that they diverged from their closest relatives [*Eleutherodactylus amplinympha* ([Kaiser et al., 1994](#)), *E. johnstonei*, *E. martinicensis*, and *Eleutherodactylus montserratiae* ([Hedges, 2022](#))] during the Miocene. Our estimates of divergence

between the sister species on Guadeloupe based on the mtDNA dataset indicate that they last shared a common ancestor ~3.75 Mya, suggesting that *in situ* diversification coincided with the earlier stages of formation of Basse-Terre. Unfortunately, our sampling is concentrated in the geologically younger, southwestern portion of the island ([Samper et al. 2007](#)); therefore, we are unable to assess intraspecific genetic structure between older and younger volcanic regions of Basse-Terre to gain a better understanding of the geographical and temporal context of *in situ* diversification. Our modelling analyses of population demographic history based on the nuDNA dataset found support for limited migration between the species throughout their history. This pattern suggests that although the species are sympatrically distributed at present, divergence largely occurred in allopatry. Allopatric speciation is considered the dominant mechanism by which speciation occurs, even on small oceanic islands ([Mayr 1963](#), [Losos and Ricklefs 2009](#)). Volcanic activity on oceanic islands, in particular, can result in landscape barriers that fragment populations and result in periods of allopatry, even across small spatial scales, and these periods of allopatry can lead to both genetic and phenotypic divergence that might result in speciation (e.g. [Stenson et al. 2002](#), [Garrick et al. 2014](#),

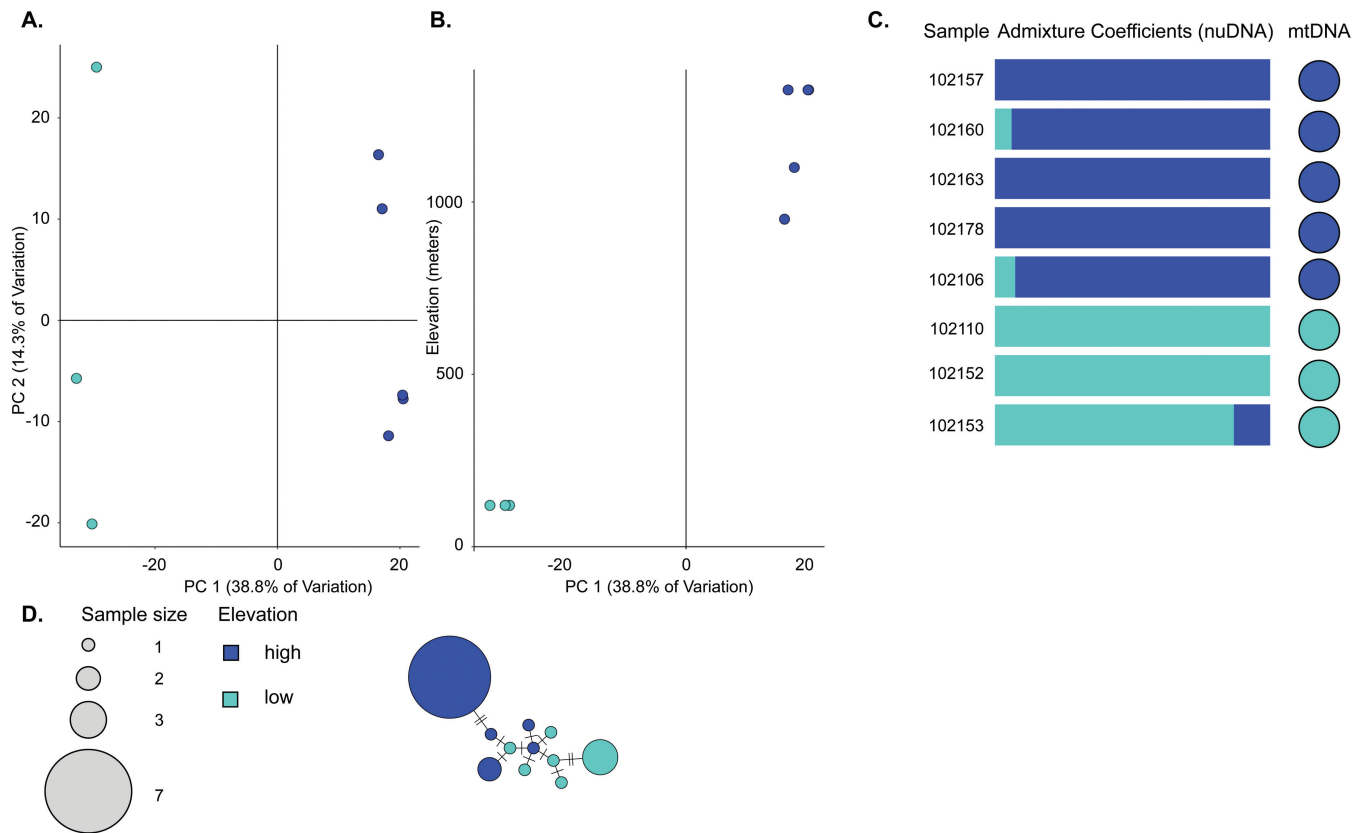


**Figure 4.** A, principal component analysis (PCA) for the *Eleutherodactylus barlagnei*-only dataset (21 627 single nucleotide polymorphisms), with samples coloured as identified in the discriminate analysis of principal components. B, principal component 1 (PC 1) axis from the PCA with respect to the elevation at which a given specimen was collected. C, sparse non-negative matrix factorization barplot depicting admixture coefficients for each specimen and its corresponding mitochondrial DNA (mtDNA) haplotype. The samples are ordered by sampling locality elevation (see [Supporting Information, Appendix](#)). D, mtDNA haplotype network for all 20 *E. barlagnei* individuals sequenced in this study. Colours correspond to high- (blue) and low-elevation (turquoise) localities. Abbreviation: nuDNA, nuclear DNA.

O'Connell et al. 2021). More comprehensive genetic sampling of the Guadeloupe *Eleutherodactylus* across their ranges would enable landscape-scale analyses and potentially reveal additional genetic variation not detected in the present sampling that would perhaps provide more insights into the geographical mode of speciation in this endemic radiation.

Secondary sympatry among sister taxa is typically associated with divergence in ecological and/or reproductive traits between the species, suggesting that differences in these traits are necessary for closely related species to coexist (Pigot and Tobias 2015, Krishnan and Tamma 2016, Friis and Milá 2020). Despite differences in ecology, morphology, and reproductive traits, previous authors have suggested that *E. barlagnei* and *E. pinchoni* might hybridize at high elevations on La Grande Soufrière, based on observations of morphologically intermediate individuals (Breuil 2002). Across our genetic assessment of 114 samples (20 *E. barlagnei* and 94 *E. pinchoni*), we found evidence of introgression in only one individual (SBH 101896 = USNM 565006) that exhibited an *E. pinchoni* mtDNA haplotype and majority assignment to *E. pinchoni* in the PCA and sNMF analysis of the nuDNA dataset. The majority assignment to *E. pinchoni* in the nuDNA analyses suggests that the individual is not a first-generation (F1) hybrid, and indeed, the morphological specimen exhibits characters diagnostic for *E. pinchoni*

(Schwartz 1967). An alternative hypothesis to explain the observed admixture of this sample is that this individual has retained a large proportion of unsorted genetic variation from the most recent common ancestor of *E. pinchoni* and *E. barlagnei*. Although incomplete lineage sorting could lead to patterns of mixed ancestry in admixture coefficients, we would expect to observe this admixture in several individuals sampled rather than only a single specimen. Furthermore, as we noted previously, the model of historical population demography indicated limited gene flow between the species over evolutionary time scales. Collectively, these results indicate that although there is not complete reproductive isolation between the species, hybridization and introgression are relatively rare, despite their largely sympatric distributions across Basse-Terre.

Although the presence of a multi-generation hybrid individual indicates that some proportion of hybrid progeny are viable and fertile (Blair 1964), the apparent low frequency of hybrid individuals in the population suggests that there might be sex differences in the viability and/or fertility of hybrid crosses (i.e. partial intrinsic reproductive isolation; Malone and Fontenot 2008) and/or that hybrids exhibit lower fitness relative to parental phenotypes owing to either ecological or sexual selection against intermediate phenotypes (i.e. extrinsic postzygotic isolation; Hatfield and Schluter 1999). The hybrid individual was

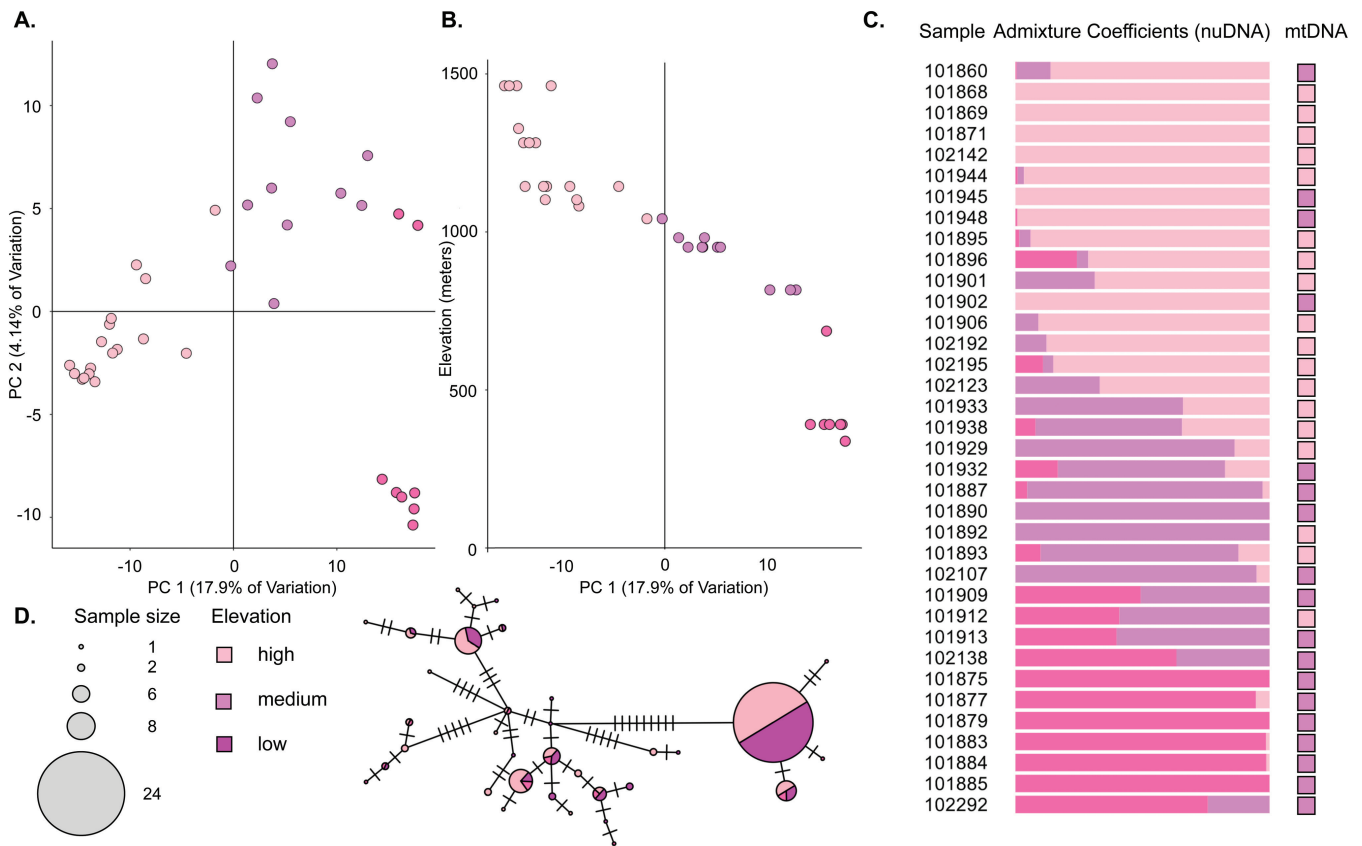


**Figure 5.** A, principal component analysis (PCA) for the *Eleutherodactylus pinchoni*-only dataset (18 217 single nucleotide polymorphisms), with samples coloured as identified in the clustering analyses. Discriminate analysis of principal components (DAPC) identified two genetic groups (shown in light and medium pink). The individuals coloured in dark pink belong to the medium pink group in the DAPC analysis and exhibited >50% assignment to the third genetic group identified in the sparse non-negative matrix factorization (sNMF) analysis. B, principal component 1 (PC 1) axis from the PCA with respect to the elevation at which a given specimen was collected. C, sNMF barplot depicting admixture coefficients for each specimen and its corresponding mitochondrial DNA (mtDNA) haplotype. The samples are ordered by sampling locality elevation (see [Supporting Information, Appendix](#)). D, mtDNA haplotype network for all 94 *E. pinchoni* individuals sequenced in this study. Colours correspond to high- (light pink), mid- (medium pink), and low-elevation (dark pink) localities. Abbreviation: nuDNA, nuclear DNA.

collected at >1100 m elevation, consistent with reports of individuals with intermediate phenotypes at higher elevation ([Breuil 2002](#)). Consequently, additional genetic screening of samples along the slopes of La Grande Soufrière might clarify whether hybridization is truly restricted to higher elevations and whether there are differences in the environmental context in these high-elevation habitats that lead to the partial breakdown of reproductive barriers.

#### Intraspecific structure along an elevational gradient

Local adaptation along elevational gradients can result in patterns of intraspecific genetic and phenotypic divergence that might eventually lead to the formation of unique evolutionary lineages ([Coyne and Orr 1998](#)). In Guadeloupe landfrogs, observations of differences in advertisement calls and coloration between low- and high-elevation populations suggest that these distinct phenotypes might be under divergent selection or represent undescribed species ([Hardy 1984, Kaiser 1993](#)). For both *E. barlagnei* and *E. pinchoni*, our data reveal genetic structure among populations from low to high elevations along the slopes of La Grande Soufrière, which is consistent with these

prior observations of phenotypic differences between populations. Our sampling for *E. barlagnei* is more limited, yet we identify clear genetic structure in the nuDNA dataset (and no shared mtDNA haplotypes), with no evidence of gene flow between the populations. This result might reflect the non-continuous nature of our sampling; however, as a stream-dwelling species, the distribution of *E. barlagnei* across the island is fragmented, and migration between suitable habitats might be more limited, resulting in more pronounced population structure (e.g. [Paz et al. 2015](#)). Unfortunately, we do not have voucher advertisement call data from low- and high-elevation populations to compare to our genetic data; however, our results highlight that this species merits further taxonomic attention. In *E. pinchoni*, we found support for two or three populations in clustering analyses of nuDNA that largely corresponded to low- and high-elevation (or low-, middle-, and high-elevation) populations, with extensive admixture between these groups at geographically proximate sites. The transition between the low- and high-elevation genetic groups at ~1000 m elevation coincides with the habitat transition from montane forest to high-elevation savannas ([Howard et al. 1980](#)) and with observations of slightly larger, more darkly

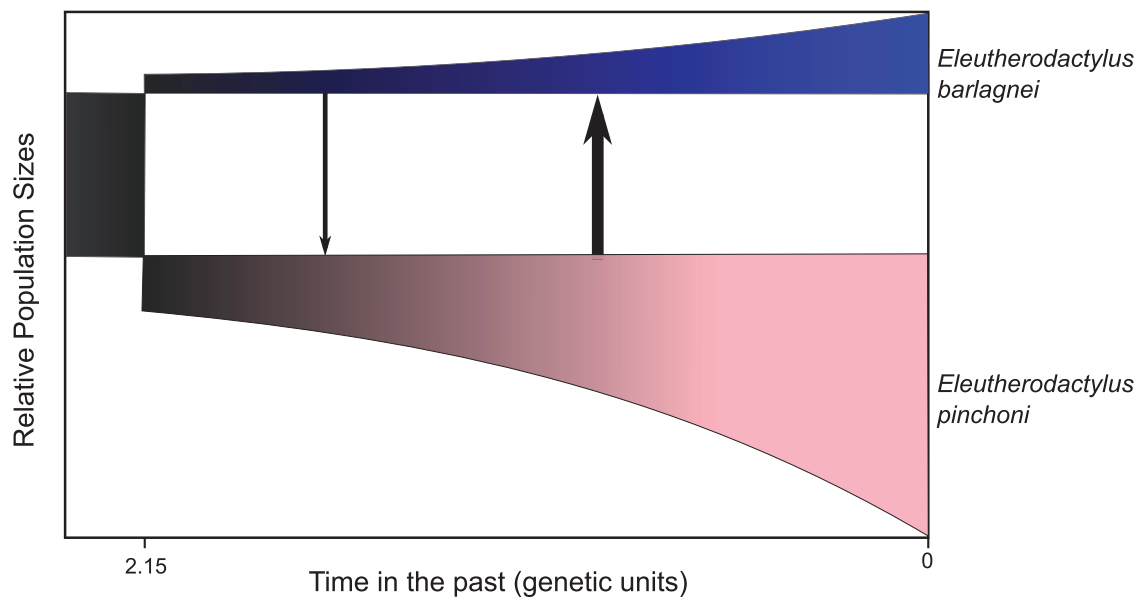


**Figure 6.** Best-fitting demographic model from GADMA using the *moments* engine after the removal of the admixed sample SBH 101896. Because of a lack of reliable genome-wide mutation rates for amphibians, the divergence times, effective population sizes, and migration rates between *Eleutherodactylus barlagnei* and *Eleutherodactylus pinchoni* are represented as scaled units. This model suggests that both species have increased in effective population size since divergence and that there has been asymmetric gene flow between the two taxa, with more migrants per generation from *E. pinchoni* into *E. barlagnei*. Results including the admixed sample SBH 101896 are shown in the [Supporting Information \(Fig. S4\)](#).

pigmented frogs (Breuil 2002). Unfortunately, we do not have robust coloration data for the individuals included in the present study to test for an association between elevation, coloration, and genetic background. Although the mtDNA phylogeny revealed two lineages in *E. pinchoni*, these haplotypes were not geographically structured, suggesting that migration and gene flow are less fragmented across low and high elevations in *E. pinchoni* than in *E. barlagnei*. This pattern does not necessarily preclude the possibility of local adaptation in *E. pinchoni* if only a few loci are under divergent selection (e.g. Muñoz *et al.* 2013, Brown *et al.* 2016, Tigano and Friesen 2016), and future studies of functional genetic variation might be fruitful once genomic resources become available in this species.

#### Population genetic structure and diversity on the slopes of an active volcano

Despite clear qualitative patterns of genetic structure with respect to elevation in *E. barlagnei* and *E. pinchoni*, our more quantitative assessments of IBD and IBE in both species were non-significant. These results might reflect limited power to detect these patterns with our present genetic sampling and the coarse resolution of environmental variables for the small geographical area that we sampled. Alternatively, these results might indicate that other factors are responsible for structuring populations. In particular, recurring volcanic eruptions of La Grande Soufrière might have played a significant role in population vicariance (e.g. Malhotra and Thorpe 2000) and perhaps even extirpation of populations (e.g. Muñoz and Hewlett 2011), as proposed for other small vertebrates on volcanic islands in the Lesser Antilles. Over the last 12 000 years alone, La Grande Soufrière has erupted 16 times, and pyroclastic flows favoured the eastern and southern sides of the volcano (Global Volcanism Program 2023). This high level

of volcanic activity might have generated temporary patchworks of vicariant barriers across the southeastern portion of the island, resulting in isolated populations. For instance, in *E. pinchoni* the sNMF analysis of nuDNA supported a third population that corresponds to samples collected from <500 m on the southeastern slopes of La Grande Soufrière. More fine-scale genetic sampling on all sides of La Grande Soufrière would enable explicit tests of whether genetic structure and secondary contact align with volcanic activity, as demonstrated in other oceanic island systems (Stenson *et al.* 2002, Garrick *et al.* 2014, O'Connell *et al.* 2021).

Another prediction of catastrophic volcanic activity on small oceanic islands is widespread declines or local extirpation of species in the immediate vicinity of habitat disturbance, as observed, for instance, for the island of Krakatoa (Whittaker *et al.* 1989, Whittaker and Jones 1994). Even smaller-scale, more localized eruptions can wipe out entire populations or communities, and harsh environmental conditions might have long-lasting effects on the availability of suitable habitats for adjacent populations to recolonize the impacted areas. For instance, following the 1995 eruption of the Soufrière Hills volcano on Montserrat (Robertson *et al.* 2000), anoles were still scarce in the exclusion zone on the southern half of the island nearly 15 years later (Muñoz and Hewlett, 2011). Population declines in response to volcanic activity might be detectable as population bottlenecks, depending on the magnitude and duration of the bottleneck (e.g. Beheregaray *et al.* 2003). For instance, surveys of the Montserrat exclusion zone in 2018 detected anoles at two localities, and serial estimates of genetic diversity in this region found similar levels of diversity pre- and post-eruption, suggesting that the exclusion zone was eventually recolonized by individuals from populations that were genetically similar to the pre-eruption inhabitants (Jung *et al.* 2024). Although we do not

have pre-eruption samples for the Guadeloupe *Eleutherodactylus* for a direct temporal comparison with post-eruption diversity, we did not find low genetic diversity in populations near the summit of La Grande Soufrière where we predicted the direct impacts of volcanic activity would be most pronounced. Instead, we found moderate to high heterozygosity across populations in both species, suggesting that the frogs were minimally impacted by eruptions and/or that populations recovered quickly.

### Insights into the process of speciation

The results here complement and reinforce our current understanding of the genetic basis of speciation, especially regarding the build-up of genomic incompatibilities (Coyne and Orr 2004; Hedges *et al.* 2015, Ravinet *et al.* 2017). Although incompatibilities segregate within species at a low level (Corbett-Detig *et al.* 2013), it is their build-up in isolation, geographical or otherwise, that eventually leads to a reproductive barrier and speciation. A survey of diverse organisms (vertebrates, invertebrates, and plants) found that the modal time to speciation was ~1–3 Myr (Hedges *et al.* 2015). Therefore, the divergence of *E. barlagnei* and *E. pinchoni* (3.75 Mya) would indicate that they are sufficiently divergent to be reproductively isolated. This agrees with our results that they are genetically distinct while being broadly sympatric, and the one hybrid that we detected is not unexpected in two closely related sympatric species. By contrast, based on the young divergence time estimated for upper- and lower-elevation populations of *E. pinchoni* (0.5 Mya), they are not expected to be distinct species, and that prediction is born out in our analyses of nuDNA data and sharing of mitochondrial haplotypes. Thus, *E. pinchoni* might represent a species in which populations accumulated some genomic incompatibilities in isolation, but then the barrier was lost, and gene flow is in the process of ‘resetting’ the speciation clock (Hedges *et al.* 2015). Further ecological and genetic research on these frogs might provide a better understanding of the early stages of speciation.

### SUPPLEMENTARY DATA

Supplementary data is available at *Zoological Journal of the Linnean Society* online.

Table S1. Voucher specimen and sampling locality information.

Figure S1. Values of each metric used to decide the best clustering threshold in ipyrad, these include inferred levels of heterozygosity, the percent of non-paralogous loci after filtering in ipyrad, and the estimated sequencing error rate from ipyrad.

Figure S2. PCA with no missing data (2,503 SNPs).

Figure S3. Mitochondrial phylogeny with complete sampling of *Eleutherodactylus barlagnei* and *E. pinchoni*.

Figure S4. Best fit demographic model from GADMA using the *moments* engine with the inclusion of the admixed sample SBH 101896.

### ACKNOWLEDGEMENTS

We thank A. Lam and L. Bonomo for their assistance with collecting data in the Academy’s Center for Comparative Genomics. We thank I. Overcast for a discussion of best practices in using IPYRAD to cluster RADseq data. S.B.H. thanks J. Fifi of the government of Guadeloupe

for export permits, J.D. Hardy for assisting him in the field, the Smithsonian’s NMNH (National Museum of Natural History) for cataloguing specimens, and R. Highton for guidance during his graduate work (when these frogs were collected). Additionally, we thank E. Langan and A. Wynn for providing access to specimens at the NMNH.

### CONFLICT OF INTEREST

None declared.

### FUNDING

We thank the U.S. National Science Foundation (8307115 and 2326013) for funding. L.A., A.B., and E.A.M. were supported by the California Academy of Science’s *Islands 2030* initiative, and analyses were conducted using the Institute for Biodiversity Science and Sustainability’s computing resources. K.P.M. was supported in part by a postdoctoral fellowship from the Fonds Wetenschappelijk Onderzoek (FWO) under grant number 1224223N.

### DATA AVAILABILITY

The data underlying this article are available in the GenBank Nucleotide Database (PQ241325 - PQ241443) and Sequence Read Archive (BioProject PRJNA1152911).

### REFERENCES

- Beheregaray LB, Ciofi C, Geist D *et al.* Genes record a prehistoric volcano eruption in the Galápagos. *Science* 2003;**302**:75. <https://doi.org/10.1126/science.1087486>
- Blair WF. Isolating mechanisms and interspecies interactions in anuran amphibians. *The Quarterly Review of Biology* 1964;**39**:334–44. <https://doi.org/10.1086/404324>
- Bouckaert R, Vaughan TG, Barido-Sottani J *et al.* BEAST 2.5: an advanced software platform for Bayesian evolutionary analysis. *PLoS Computational Biology* 2019;**15**:e1006650. <https://doi.org/10.1371/journal.pcbi.1006650>
- Bradburd G. popgenstuff: Handy Functions for PopGen Analysis in R version 0.0.0.9000. 2012. <https://github.com/gbradburd/popgenstuff>
- Breuil M. *Histoire Naturelle des Amphibiens et Reptiles terrestres de l’archipel Guadeloupéen: Guadeloupe, Saint-Martin, Saint-Barthélemy*, Vol. **54**. Paris: Patrimoines naturels, Muséum national d’Histoire naturelle, 2002.
- Brown RP, Paterson S, Risse J. Genomic signatures of historical allopatry and ecological divergence in an Island Lizard. *Genome Biology and Evolution* 2016;**8**:3618–26. <https://doi.org/10.1093/gbe/evw268>
- Cambers G. Lesser Antilles. In: Bird ECF (ed.), *Encyclopedia of the World’s Coastal Landforms*. Dordrecht: Springer Netherlands, 2010, 299–310. [https://doi.org/10.1007/978-1-4020-8639-7\\_50](https://doi.org/10.1007/978-1-4020-8639-7_50)
- Carson HL, Lockwood JP, Craddock EM. Extinction and recolonization of local populations on a growing shield volcano. *Proceedings of the National Academy of Sciences of the United States of America* 1990;**87**:7055–7. <https://doi.org/10.1073/pnas.87.18.7055>
- Carstens B, Lemmon AR, Lemmon EM. The promises and pitfalls of next-generation sequencing data in phylogeography. *Systematic Biology* 2012;**61**:713–5. <https://doi.org/10.1093/sysbio/sys050>
- Corbett-Detig RB, Zhou J, Clark AG *et al.* Genetic incompatibilities are widespread within species. *Nature* 2013;**504**:135–7. <https://doi.org/10.1038/nature12678>
- Costello M, Fleharty M, Abreu J *et al.* Characterization and remediation of sample index swaps by non-redundant dual indexing on massively parallel sequencing platforms. *BMC Genomics* 2018;**19**:332. <https://doi.org/10.1186/s12864-018-4703-0>
- Coyne JA, Orr HA. Speciation: a catalogue and critique of species concepts. *Philosophy of Biology: an Anthology* 2004:272–92.

- Coyne JA, Orr HA. The evolutionary genetics of speciation. *Philosophical Transactions of the Royal Society of London, Series B: Biological Sciences* 1998;**353**:287–305. <https://doi.org/10.1098/rstb.1998.0210>
- Dammerman KW. *The Agricultural Zoology of the Malay Archipelago*. Amsterdam: J. H. de Bussy, 1929.
- Danecek P, Auton A, Abecasis G et al.; Genomes Project Analysis Group. The variant call format and VCFtools. *Bioinformatics* 2011;**27**:2156–8. <https://doi.org/10.1093/bioinformatics/btr330>
- Darriba D, Taboada GL, Doallo R et al. jModelTest 2: more models, new heuristics and high-performance computing. *Nature Methods* 2012;**9**:772. <https://doi.org/10.1038/nmeth.2109>
- Dray S, Dufour AB. The ade4 package: implementing the duality diagram for ecologists. *Journal of Statistical Software* 2007;**22**:1–20. <https://doi.org/10.18637/jss.v022.i04>
- Eaton DAR, Overcast I. ipyrad: interactive assembly and analysis of RADseq datasets. *Bioinformatics* 2020;**36**:2592–4. <https://doi.org/10.1093/bioinformatics/btz966>
- Edgar RC. MUSCLE: multiple sequence alignment with high accuracy and high throughput. *Nucleic Acids Research* 2004;**32**:1792–7. <https://doi.org/10.1093/nar/gkh340>
- Ferrier S, Manion G, Elith J et al. Using generalized dissimilarity modeling to analyse and predict patterns of beta diversity in regional biodiversity assessment. *Diversity and Distributions* 2007;**13**:252–64. <https://doi.org/10.1111/j.1472-4642.2007.00341.x>
- Feuillet N, Manighetti I, Taponnier P et al. Arc parallel extension and localization of volcanic complexes in Guadeloupe, Lesser Antilles. *Journal of Geophysical Research, Solid Earth* 2002;**107**:ETG 3–1–ETG 3–29. <https://doi.org/10.1029/2001JB000308>
- Frichot E, François O. LEA: an R package for landscape and ecological association studies. *Methods in Ecology and Evolution* 2015;**6**:925–9. <https://doi.org/10.1111/2041-210x.12382>
- Friis G, Milá B. Change in sexual signalling traits outruns morphological divergence across an ecological gradient in the post-glacial radiation of the songbird genus *Junco*. *Journal of Evolutionary Biology* 2020;**33**:1276–93. <https://doi.org/10.1111/jeb.13671>
- García-Rodríguez A, Guarnizo CE, Crawford AJ et al. Idiosyncratic responses to drivers of genetic differentiation in the complex landscapes of Isthmian Central America. *Heredity* 2021;**126**:251–65. <https://doi.org/10.1038/s41437-020-00376-8>
- Garrick RC, Benavides E, Russello MA et al. Lineage fusion in Galápagos giant tortoises. *Molecular Ecology* 2014;**23**:5276–90. <https://doi.org/10.1111/mec.12919>
- Global Volcanism Program. Soufrière Guadeloupe (360060) in Holocene Volcanoes of the World (v.5.1.5). 2023. Distributed by Smithsonian Institution, compiled by Venzke, E. <https://doi.org/10.5479/si.GVP.VOTWS-2023.5.1>
- Grant EHC, Mulder KP, Brand AB et al. Speciation with gene flow in a narrow endemic West Virginia cave salamander (*Gyrinophilus subterraneus*). *Conservation Genetics* 2022;**23**:727–44. <https://doi.org/10.1007/s10592-022-01445-7>
- Hardy JD. *Frog Mountain: Preliminary comments on the genus Eleutherodactylus on the island of Guadeloupe, West Indies*, Vol. 21. Baltimore: Maryland Herpetological Society, Department of Herpetology, Natural History Society of Maryland, 1984, 27–33.
- Harvey MG, Judy CD, Seeholzer GF et al. Similarity thresholds used in DNA sequence assembly from short reads can reduce the comparability of population histories across species. *PeerJ* 2015;**3**:e895. <https://doi.org/10.7717/peerj.895>
- Hatfield T, Schluter D. Ecological speciation in sticklebacks: environment-dependent hybrid fitness. *Evolution* 1999;**53**:866–73. <https://doi.org/10.1111/j.1558-5646.1999.tb05380.x>
- Hedges SB. Evolution and biogeography of West Indian frogs of the genus *Eleutherodactylus*: slow-evolving loci and the major groups. In: Woods CA (ed.), *Biogeography of the West Indies: Past, Present, and Future*. Gainesville: Sandhill Crane Press, 1989, 305–70.
- Hedges SB, Duellman WE, Heinicke MP. New World direct-developing frogs (Anura: Terrarana): molecular phylogeny, classification, biogeography, and conservation. *Zootaxa* 2008;**1737**:1–182. <https://doi.org/10.11646/zootaxa.1737.1.1>
- Hedges SB, Marin J, Suleski M et al. Tree of life reveals clock-like speciation and diversification. *Molecular Biology and Evolution* 2015;**32**:835–45. <https://doi.org/10.1093/molbev/msv037>
- Heinicke MP, Duellman WE, Hedges SB. Major Caribbean and Central American frog faunas originated by ancient oceanic dispersal. *Proceedings of the National Academy of Sciences of the United States of America* 2007;**104**:10092–7. <https://doi.org/10.1073/pnas.0611051104>
- Hoang DT, Chernomor O, Von Haeseler A et al. UFBoot2: improving the ultrafast bootstrap approximation. *Molecular Biology and Evolution* 2018;**35**:518–22. <https://doi.org/10.1093/molbev/msx281>
- Howard RA, Howard RA, Portecop J et al. The post-eruptive vegetation of La Soufrière, Guadeloupe, 1977–1979. *Journal of the Arnold Arboretum* 1980;**61**:749–64. <https://doi.org/10.5962/p.185898>
- Ilut DC, Nydam ML, Hare MP. Defining loci in restriction-based reduced representation genomic data from nonmodel species: sources of bias and diagnostics for optimal clustering. *Biomed Research International* 2014;**2014**:675158. <https://doi.org/10.1155/2014/675158>
- Imbert D, Labbé P, Rousteau A. Hurricane damage and forest structure in Guadeloupe, French West Indies. *Journal of Tropical Ecology* 1996;**12**:663–80. <https://doi.org/10.1017/s026646740000986x>
- Jombart T. *ade4*: an R package for the multivariate analysis of genetic markers. *Bioinformatics* 2008;**24**:1403–5. <https://doi.org/10.1093/bioinformatics/btn129>
- Jouanous J, Long W, Ragsdale AP et al. Inferring the joint demographic history of multiple populations: beyond the diffusion approximation. *Genetics* 2017;**206**:1549–67. <https://doi.org/10.1534/genetics.117.200493>
- Jung C, Frederick JH, Graham NR et al. Environmentally associated colour divergence does not coincide with population structure across Lesser Antillean anoles. *Biological Journal of the Linnean Society* 2024;blae047. <https://doi.org/10.1093/biolinnean/blae047>
- Kaiser H. The trade-mediated introduction of *Eleutherodactylus martinicensis* (Anura: Leptodactylidae) on St. Barthélemy, French Antilles, and its implications for lesser Antillean biogeography. *Journal of Herpetology* 1992;**26**:264–73. <https://doi.org/10.2307/1564880>
- Kaiser H. *Systematics and Biogeography of Eastern Caribbean Frogs*. Montreal, Canada: McGill University, 1993.
- Kalyaanamoorthy S, Minh BQ, Wong TK et al. ModelFinder: fast model selection for accurate phylogenetic estimates. *Nature Methods* 2017;**14**:587–9. <https://doi.org/10.1038/nmeth.4285d>
- Karger DN, Conrad O, Böhrner J et al. Climatologies at high resolution for the Earth's land surface areas. *Scientific Data* 2017;**4**:170122. <https://doi.org/10.1038/sdata.2017.122>
- Krishnan A, Tamma K. Divergent morphological and acoustic traits in sympatric communities of Asian barbets. *Royal Society Open Science* 2016;**3**:160117. <https://doi.org/10.1098/rsos.160117>
- Losos JB, Ricklefs RE. Adaptation and diversification on islands. *Nature* 2009;**457**:830–6. <https://doi.org/10.1038/nature07893>
- Malhotra A, Thorpe RS. The dynamics of natural selection and vicariance in the Dominican anole: patterns of within-island molecular and morphological divergence. *Evolution* 2000;**54**:245–58.
- Malone JH, Fontenot BE. Patterns of reproductive isolation in toads. *PLoS One* 2008;**3**:e3900. <https://doi.org/10.1371/journal.pone.0003900>
- Manion G, Lisk M, Ferrier S et al. gdm: Functions for Generalized Dissimilarity Modeling. *R package 1*: 7. 2016. <https://github.com/fitzLab-AL/gdm/>
- Marske KA. Effects of volcanic ash on the forest canopy insects of Montserrat. *West Indies Environmental Entomology* 2007;**36**:817–25.
- Massaro S, Dioguardi F, Sandri L et al. Testing gas dispersion modelling: a case study at La Soufrière volcano (Guadeloupe, Lesser Antilles). *Journal of Volcanology and Geothermal Research* 2021;**417**:107312. <https://doi.org/10.1016/j.jvolgeores.2021.107312>
- Mayr E. *Animal Species and Evolution*. Cambridge, MA and London, UK: Harvard University Press, 1963. <https://doi.org/10.4159/harvard.9780674865327>
- McCartney-Melstad E, Gidiş M, Shaffer HB. An empirical pipeline for choosing the optimal clustering threshold in RADseq studies. *Molecular Ecology Resources* 2019;**19**:1195–204. <https://doi.org/10.1111/1755-0998.13029>

- Minh BQ, Schmidt HA, Chernomor O *et al.* IQ-TREE 2: new models and efficient methods for phylogenetic inference in the genomic era. *Molecular Biology and Evolution* 2020;**37**:1530–4. <https://doi.org/10.1093/molbev/msaa015>
- Muñoz MM, Crawford NG, McGreevy TJ Jr *et al.* Divergence in coloration and ecological speciation in the *Anolis marmoratus* species complex. *Molecular Ecology* 2013;**22**:2668–82. <https://doi.org/10.1111/mec.12295>
- Muñoz MM, Hewlett J. Ecological consequences of continual volcanic activity on the Lizard, *Anolis lividus*, from Montserrat. *Herpetological Review* 2011;**42**:160–5.
- Noskova E, Abramov N, Iliutkin S *et al.* GADMA2: more efficient and flexible demographic inference from genetic data. *GigaScience* 2023;**12**:giad059. <https://doi.org/10.1093/gigascience/giad059>
- Noskova E, Ulyantsev V, Koepfli KP *et al.* GADMA: genetic algorithm for inferring demographic history of multiple populations from allele frequency spectrum data. *GigaScience* 2020;**9**:giaa005. <https://doi.org/10.1093/gigascience/giaa005>
- O'Connell KA, Prates I, Scheinberg LA *et al.* Speciation and secondary contact in a fossorial island endemic, the São Tomé caecilian. *Molecular Ecology* 2021;**30**:2859–71. <https://doi.org/10.1111/mec.15928>
- Paradis E. pegas: an R package for population genetics with an integrated-modular approach. *Bioinformatics* 2010;**26**:419–20. <https://doi.org/10.1093/bioinformatics/btp696>
- Paz A, Ibáñez R, Lips KR *et al.* Testing the role of ecology and life history in structuring genetic variation across a landscape: a trait-based phylogeographic approach. *Molecular Ecology* 2015;**24**:3723–37. <https://doi.org/10.1111/mec.13275>
- Peterson BK, Weber JN, Kay EH *et al.* Double digest RADseq: an inexpensive method for *de novo* SNP discovery and genotyping in model and non-model species. *PLoS One* 2012;**7**:e37135. <https://doi.org/10.1371/journal.pone.0037135>
- Pigot AL, Tobias JA. Dispersal and the transition to sympatry in vertebrates. *Proceedings. Biological Sciences* 2015;**282**:20141929. <https://doi.org/10.1098/rspb.2014.1929>
- R Core Team. R: *The R Project for Statistical Computing*. 2008.
- Rambaut A, Drummond AJ, Xie D *et al.* Posterior summarization in Bayesian phylogenetics using Tracer 1.7. *Systematic Biology* 2018;**67**:901–4. <https://doi.org/10.1093/sysbio/syy032>
- Ravinet M, Faria R, Butlin RK *et al.* Interpreting the genomic landscape of speciation: a road map for finding barriers to gene flow. *Journal of Evolutionary Biology* 2017;**30**:1450–77. <https://doi.org/10.1111/jeb.13047>
- Robertson REA, Aspinall WP, Herd RA *et al.* The 1995–1998 Eruption of the Soufriere Hills Volcano, Montserrat, WI. *Philosophical Transactions: Mathematical, Physical and Engineering Sciences* 2000;**358**:1619–37. <https://doi.org/10.1098/rsta.2000.0607>
- Rodríguez-Ezpeleta N, Bradbury IR, Mendibil I *et al.* Population structure of Atlantic mackerel inferred from RAD-seq-derived SNP markers: effects of sequence clustering parameters and hierarchical SNP selection. *Molecular Ecology Resources* 2016;**16**:991–1001. <https://doi.org/10.1111/1755-0998.12518>
- Roesch Goodman K, Welter SC, Roderick GK. Genetic divergence is decoupled from ecological diversification in the Hawaiian Nesosydne planthoppers: divergence decoupled from diversification. *Evolution* 2012;**66**:2798–814. <https://doi.org/10.1111/j.1558-5646.2012.01643.x>
- Rosenblum EB. Convergent evolution and divergent selection: lizards at the white sands ecotone. *The American Naturalist* 2006;**167**:1–15. <https://doi.org/10.1086/498397>
- Samper A, Quidelleur X, Lahitte P *et al.* Timing of effusive volcanism and collapse events within an oceanic arc island: Basse-Terre, Guadeloupe archipelago (Lesser Antilles Arc). *Earth and Planetary Science Letters* 2007;**258**:175–91. <https://doi.org/10.1016/j.epsl.2007.03.030>
- Schwartz A. Frogs of the genus *Eleutherodactylus* in the Lesser Antilles. *Studies on the Fauna of Curaçao and other Caribbean Islands* 1967;**24**:1–62.
- Shafer ABA, Peart CR, Tusso S *et al.* Bioinformatic processing of RAD-seq data dramatically impacts downstream population genetic inference. *Methods in Ecology and Evolution* 2017;**8**:907–17. <https://doi.org/10.1111/2041-210X.12700>
- Stenson AG, Malhotra A, Thorpe RS. Population differentiation and nuclear gene flow in the Dominican anole (*Anolis oculatus*). *Molecular Ecology* 2002;**11**:1679–88. <https://doi.org/10.1046/j.1365-294x.2002.01564.x>
- Stoler N, Nekrutenko A. Sequencing error profiles of Illumina sequencing instruments. *NAR Genomics and Bioinformatics* 2021;**3**:lqab019. <https://doi.org/10.1093/nargab/lqab019>
- Stuart-Fox D, Moussalli A. Selection for social signalling drives the evolution of chameleon colour change. *PLoS Biology* 2008;**6**:e25. <https://doi.org/10.1371/journal.pbio.0060025>
- Stuart-Fox DM, Ord TJ. Sexual selection, natural selection and the evolution of dimorphic coloration and ornamentation in agamid lizards. *Proceedings of the Royal Society of London. Series B: Biological Sciences* 2004;**271**:2249–55. <https://doi.org/10.1098/rspb.2004.2802>
- Terhorst J, Song YS. Fundamental limits on the accuracy of demographic inference based on the sample frequency spectrum. *Proceedings of the National Academy of Sciences of the United States of America* 2015;**112**:7677–82. <https://doi.org/10.1073/pnas.1503717112>
- Tigano A, Friesen VL. Genomics of local adaptation with gene flow. *Molecular Ecology* 2016;**25**:2144–64. <https://doi.org/10.1111/mec.13606>
- Vavrek R, Matthew J. fossil: palaeoecological and palaeogeographical analysis tools. *Palaeontologia Electronica* 2011;**14**:1T. [http://palaeo-electronica.org/2011\\_1/238/index.html](http://palaeo-electronica.org/2011_1/238/index.html)
- Velo-Antón G, Burrows PA, Joglar RL *et al.* Phylogenetic study of *Eleutherodactylus coqui* (Anura: Leptodactylidae) reveals deep genetic fragmentation in Puerto Rico and pinpoints origins of Hawaiian populations. *Molecular Phylogenetics and Evolution* 2007;**45**:716–28. <https://doi.org/10.1016/j.ympev.2007.06.025>
- Whittaker RJ, Bush MB, Richards K. Plant recolonization and vegetation succession on the Krakatau Islands, Indonesia. *Ecological Monographs* 1989;**59**:59–123. <https://doi.org/10.2307/2937282>
- Whittaker RJ, Jones SH. The role of frugivorous bats and birds in the rebuilding of a tropical forest ecosystem, Krakatau, Indonesia. *Journal of Biogeography* 1994;**21**:245–58. <https://doi.org/10.2307/2845528>
- Yuan ML, Frederick JH, McGuire JA *et al.* Endemism, invasion, and overseas dispersal: the phylogeographic history of the Lesser Antillean frog, *Eleutherodactylus johnstonei*. *Biological Invasions* 2022;**24**:2707–22. <https://doi.org/10.1007/s10530-022-02803-9>
- Zlotnicki J, Boudon G, Le Mouél JL. The volcanic activity of La Soufrière of Guadeloupe (Lesser Antilles): structural and tectonic implications. *Journal of Volcanology and Geothermal Research* 1992;**49**:91–104. [https://doi.org/10.1016/0377-0273\(92\)90006-y](https://doi.org/10.1016/0377-0273(92)90006-y)